Structural Monitoring and Maintenance, *Vol. 7, No. 2 (2020) 201-226*
DOI: https://doi.org/10.12989/smm.2020.7.2.201

Numerical study on the performance of semicircular and rectangular submerged breakwaters

Mohammad Barzegar[1a] and D. Palaniappan*[2]

[1]*Department of Physical & Environmental Sciences, Texas A&M University, Corpus Christi, 6300 Ocean Drive, Corpus Christi, TX 78412*
[2]*Department of Mathematics & Statistics, Texas A&M University, Corpus Christi, 6300 Ocean Drive, Corpus Christi, TX 78412*

(Received January 23, 2020, Revised May 20, 2020, Accepted June 15, 2020)

Abstract. A systematic numerical comparative study of the performance of semicircular and rectangular submerged breakwaters interacting with solitary waves is the basis of this paper. To accomplish this task, Nwogu's extended Boussinesq model equations are employed to simulate the interaction of the wave with breakwaters. The finite difference technique has been used to discretize the spatial terms while a fourth-order predictor-corrector method is employed for time discretization in our numerical model. The proposed computational scheme uses a staggered-grid system where the first-order spatial derivatives have been discretized with fourth-order accuracy. For validation purposes, five test cases are considered and numerical results have been successfully compared with the existing analytical and experimental results. The performances of the rectangular and semicircular breakwaters have been examined in terms of the wave reflection, transmission, and dissipation coefficients (RTD coefficients) denoted by K_R, K_T, K_D. The latter coefficient K_D emerges due to the non-energy conserving K_R and K_T,. Our computational results and graphical illustrations show that the rectangular breakwater has higher reflection coefficients than semicircular breakwater for a fixed crest height, but as the wave height increases, the two reflection coefficients approach each other. On the other hand, the rectangular breakwater has larger dissipation coefficients compared to that of the semicircular breakwater and the difference between them increases as the height of the crest increases. However, the transmission coefficient for the semicircular breakwater is greater than that of the rectangular breakwater and the difference in their transmission coefficients increases with the crest height. Quantitatively, for rectangular breakwaters the reflection coefficients K_R are 5-15% higher while the diffusion coefficients K_D are 3-23% higher than that for the semicircular breakwaters, respectively. The transmission coefficients K_T for rectangular breakwater shows the better performance up to 2.47% than that for the semicircular breakwaters. Based on our computational results, one may conclude that the rectangular breakwater has a better overall performance than the semicircular breakwater. Although the model equations are non-dissipative, the non-energy conserving transmission and reflection coefficients due to wave-breakwater interactions lead to dissipation type contribution.

Keywords: Nwogu's extended Boussinesq equations; semicircular breakwater; rectangular breakwater; RTD coefficients; performance; finite difference method

*Corresponding author, Associate Professor, E-mail: devanayagam.palaniappan@tamucc.edu
[a] Ph.D. Student, E-mail: Mbarzegarpaiinlamouk@Islander.tamucc.edu

http://www.techno-press.org/?journal=smm&subpage=7 ISSN: 2288-6605 (Print), 2288-6613 (Online)

1. Introduction

The protection of beaches and ports from erosion due to sea waves is a growing challenge for coastal and marine engineers. Offshore and onshore constructions of submerged barriers and artificial reefs depend heavily on many parameters especially, the incoming wave height. In order to control sediment transportation and structural damages due to wave interactions, it is crucial that engineers look for a variety of ways to reduce incoming wave heights. Breakwaters are widely recognized as the most popular beach structures that provide appropriate tools to maintain calm beach areas reasonably well.

The most common breakwaters are the structures whose crests emerge from the surface. In areas where visual limitation exists and breakwaters should not be visible, the submerged breakwaters are utilized with their crests located under the water. Although the submerged breakwaters are less capable compared to that of emerged ones and are also inconvenient for navigation purposes, they are widely used for economic benefits. These structures are suitable tools for protecting beach areas against small and relatively high waves. Waves may break through colliding with submerged breakwaters and/or their height gets reduced as a result of friction and permeability in the breakwaters. For a better understanding of the performance of the breakwaters of various shapes, physicists and engineers need to identify fundamental wave characteristics when passing over a breakwater.

Theoretical studies modeling solitary wave passing over shore obstacles were initiated by Johnson (1972) and Tappert and Zabusky (1971) by analytical examination of the governing equations, Subsequently, several other investigations followed and experiments were conducted to validate proposed theories (Losada and Medina 1989, Mei 1985, Ghiasian *et al.* 2019, Bogucki *et al*. 2020). One of the major findings of those earlier studies is that a typical submerged bar has a meaningful effect on reflection and transmission (e.g., Newman 1965, Ketabdari *et al*. 2015) of the impinging waves. Indeed, Beji and Battjes (1993, 1994) and Grilli and Martin (1994) have analyzed submerged bar type of obstacles both numerically and experimentally that led to similar conclusions.

To understand the phenomenon of wave passisdng and interaction with shore barriers more realistically, extensive field studies have been carried out on Florida plan beach by Dean *et al*. (1997). This field investigation included a supervisory community program on the beach executed using positioning measuring instruments of wave parameters installed around submerged breakwaters on the beach area. Practically significant results have been recorded that are relevant to operational mechanisms with shore obstacles. Specifically, the field results revealed that reduction of wave height has happened about 5% for the small waves and 15% for the high waves.

The primary engineering concerns for water solitary waves propagating and interacting with breakwaters are wave reflection, transmission, and dissipation (RTD) coefficients. Allsop (1983) and Wang *et al.* (2019), among others, analyzed wave energy transmission over the submerged breakwaters. The studies conducted by Dick and Brebner (1968) on submerged breakwaters showed that these structures with crest height close to the sea surface are able to absorb 50% wave energy. The observations of these studies on the shore obstacles emphasized the knowledge of evaluating the corresponding RTD coefficients. A comprehensive study in this related topic has been conducted by Lin (2004) on the RTD coefficients involving rectangular obstacles. In the cited work, a numerical model was used to simulate the interaction between solitary waves and rectangular obstacles for different combinations of length (L) and height (D) of the breakwater. These coefficients were calculated and tabulated for engineering applications for various L/h and D/h (h = constant water depth). In particular, Lin showed that wave breaking and vortex shedding are the main reasons

behind energy dissipation that reduces wave transmission (see Lin 2004).

Subsequently, Lin and Karunarathna (2007) provided an estimation of the RTD coefficients of solitary waves over porous obstacles. Laboratory studies for characterizing wave reflection coefficients in semicircular submerged breakwaters have been performed by Young and Testik (2011, 2009). The results are of great interest to marine engineers for the primary design of breakwaters of various shapes. By developing a Reynolds Averaged Navier-Stokes model, Hsu *et al*. (2004) managed to simulate the dissipation of passing waves over submerged breakwaters and Raman *et al.* (1997) expressed wave transmission coefficients in terms of wave energy and the total power of the incident wave. Since the geometry of the breakwaters affects the wave kinematics, wave breaking style and also the RTD coefficients, considerable attention was focused on this area to explore further implications by several researchers (see, for instance, Lee and Mizutani 2008, Yuan and Tao 2003). The cited papers analyzed submerged breakwaters' geometries and their effects on flow parameters. Among various types of submerged breakwaters, the structure with semicircular, rectangular and trapezoidal shapes have been found more applicable as noted in by Cooker *et al*. (1990) and Tsai *et al*. (2005).

The wave propagation with triangular structures has been discussed by Seabra-Santos *et al*. (1987), Wu and Hsiao (2013) by using numerical and experimental techniques to investigate the interaction between non-breaking solitary waves and rectangular submerged breakwaters. In their study, time histories of surface elevation and the spatial distributions of free surface displacement were obtained, and the results showed that at a constant water depth the turbulent intensity values increase with an increase of solitary wave height. Although the wide range of studies has been conducted on the effect of breakwater geometry on its performance, investigations on this topic are considered highly significant and as a result, there is a growing interest in the modern era (e.g., Xie and Liu 2013, Ji *et al*. 2016, Wu *et al*. 2017).

As narrated in the preceding paragraphs while wave interactions with various shapes of barriers are investigated on numerous occasions a systematic study on the performance comparison is still lacking. Motivated by this, in the present paper we choose a numerical study to compare the performance of semicircular and rectangular submerged breakwaters. The analysis is carried out by investigating the interaction of solitary waves and breakwaters. The governing equations used for simulating solitary waves in the present study are the Nwogu's extended Boussinesq equations (Nwogu 1993). The nonlinear equations along with solid wall and spongy boundary conditions are solved by the finite difference method. The numerical scheme involves appropriate discretization of the time and space variables. To show the accuracy of our finite difference numerical scheme, the propagation of a solitary wave is modeled and solved with a constant depth, the run-up of a solitary wave on a beach with different slopes, as well as the wave run up on a slope, and its reflection from a solid wall. Later, the capability of the model to simulate rectangular and semicircular breakwaters is studied using two different tests. The results of the considered tests are compared against previous analytical, numerical, and experimental findings. Finally, by applying various heights for solitary wave and submerged breakwater crests, the RTD coefficients are obtained for each of the submerged breakwaters and the performance of these submerged breakwaters is analyzed and compared. Our analysis provides a systematic numerical study leading to a better understanding of the comparative performance of the rectangular and semicircular breakwaters while interacting with solitary waves.

2. Governing equations

Submerged breakwaters are commonly installed offshore and at intermediate water depths. Simulation of the interaction between waves and submerged breakwaters requires model equations which are able to mimic wave transfer from deep water to shallow water. Among equations that are useful for numerical simulation of this type, the Boussinesq equations are of great interest and have been employed successfully. The first generalization incorporating variable depth have been extracted by Peregrine (1967), known as standard Boussinesq equations. Since the equations proposed by Peregrine has the ability to model waves in shallow waters, efforts have been made by several researchers to develop the equations for deep waters (Beji and Nadaoka 1996, Madsen and Sorensen 1991, Madsen and Sørensen 1992). Another extension of these equations proposed by Nwogu (1993) became widely popular among engineers because of their relatively simple form and ability to simulate nonlinear and dispersion terms (Zhang and Qiao 2017, Lee and Jung 2018). In Nwogu's extended Boussinesq equations, velocity is considered as a dependent variable at arbitrary depths. We choose the latter equations in our present study. Nwogu's two-dimensional extended Boussinesq equations are continuity and momentum equations presented as follows (Nwogu 1993).

$$\eta_t + \nabla.[(h+\eta)U] + \nabla.\left\{\left(\frac{Z_\alpha^2}{2} - \frac{h^2}{6}\right)h\nabla(\nabla.U) + \left(Z_\alpha + \frac{h}{2}\right)h\nabla[\nabla.(hU)]\right\} = 0 \quad (1)$$

$$U_t + g\nabla\eta + (U\ .\ \nabla)U + Z_\alpha\{\frac{Z_\alpha}{2}\nabla(\nabla.U_t) + \nabla[\nabla.(hU_t)]\} = 0 \quad (2)$$

where η stands for surface elevation, h is water depth, $U = (u, v)$ is the horizontal velocity at an arbitrary depth $Z_\alpha = 0.531\ h$, $\nabla = (\frac{\partial}{\partial x}, \frac{\partial}{\partial y})$ stands for gradient, the time differentiation is denoted by a subscript and g is the gravity acceleration. Eqs. (1) and (2) can be rewritten for the one-dimensional case in the form (Lin and Man 2005)

$$\frac{\partial\eta}{\partial t} + \frac{\partial}{\partial x}[(h+\eta)u] + \frac{\partial}{\partial x}\left[\left(\frac{\left(\frac{Z_\alpha}{h}\right)^2}{2} - \frac{1}{6}\right)h^3\left(\frac{\partial^2 u}{\partial x^2}\right) + (\frac{Z_\alpha}{h} + \frac{1}{2}\ \ )h^2\left(\frac{\partial^2(hu)}{\partial x^2}\right)\right] = 0 \quad (3)$$

$$\frac{\partial u}{\partial t} + g\frac{\partial\eta}{\partial x} + u\frac{\partial u}{\partial x} + \frac{(\frac{Z_\alpha}{h})^2}{2}h^2\frac{\partial}{\partial t}\left(\frac{\partial^2 u}{\partial x^2}\right) + Z_\alpha\frac{\partial}{\partial t}\left(\frac{\partial^2(hu)}{\partial x^2}\right) = 0 \quad (4)$$

In the following section, we describe our numerical scheme using finite difference for discretizing space and time variables in the governing equations (3) and (4) and provide boundary conditions.

3. Numerical model

Following the approach adopted by Lin and Man (2007) and Wei and Kirby (1995), for the first-order spatial derivatives we use the fourth-order accuracy of the central difference scheme while for time integration, the fourth-order Adams predictor-corrector scheme is implemented. This choice causes numerical dissipation and dispersion that are of a desired high order and offers a better mass conversion in long-term simulations.

3.1 Discretization of the governing equations

In order to solve the governing equations numerically using Adams predictor-corrector scheme, the simplified forms of (3) and (4) are written to be

$$\eta_t = \ E(\eta, u) \tag{5}$$

$$u_t + h[b_1 h\left(\frac{\partial^2 u_t}{\partial x^2}\right) + b_2\left(\frac{\partial^2 (hu_t)}{\partial x^2}\right)] = \ F(\eta, u) \tag{6}$$

Now the left-hand side of (6) can be expressed as follows:

$$[U(u)]_t = [\ u + h[\ b_1 h\ u_{xx} + b_2 (hu)_{xx}]]_t \tag{7}$$

The quantities E and F on the right-hand side of (6) are the dependent functions of the variables u and η stated in the following equations:

$$E(\eta, u, v) = -[(h+\eta)u]_x - \{\ \alpha_1 h^3 (u_{xx}) + \alpha_2 h^2 [(hu)_{xx}\ \}_x \tag{8}$$

$$F(\eta, u) = -g\eta_x - \frac{1}{2}(u^2)_x \tag{9}$$

where $\alpha_1,\ \alpha_2,\ b_1,$ and b_2 are defined as

$$\alpha_1 = \ \frac{\left(\frac{Z_\alpha}{h}\right)^2}{2} - \frac{1}{6} \quad ; \quad \alpha_2 = \left(\frac{Z_\alpha}{h}\right) + \frac{1}{2} \quad ; \quad b_1 = \frac{\left(\frac{Z_\alpha}{h}\right)^2}{2} \quad ; \quad b_2 = \left(\frac{Z_\alpha}{h}\right) \tag{10}$$

Various terms in the continuity and momentum equations are discretized in the spatial domain based on a staggered grid system. Accordingly, water surface elevation (η) and water depth (h) are placed at the cell center and the velocity vector component (u) is located on the interfaces of the cell, as shown in Fig. 1. Scalar values of η and h on the interfaces of the cell are obtained by linear interpolation. Cells are sized equally (Δx) and are referred to by subscript indices $i = 1,2,\dots,m$ increasing in the x direction. Time integration is applied to the equations through the predictor-corrector method introduced by Wei and Kirby (1995). In the predictor step, values of u and η are obtained with respect to the prior time steps using the explicit third-order Adams-Bashforth method. The time step is expressed as Δt and superscript n in Eqs. (11) and (12) refers to the present time. Eqs. (5) and (6) are rewritten as follows:

$$\eta_{i,j}^{n+1} = \eta_{i,j}^{n} + \frac{\Delta t}{12}[23E_{i,j}^{n} - 16E_{i,j}^{n-1} + 5E_{i,j}^{n-2}] \tag{11}$$

$$U_{i+1/2,j}^{n+1} = U_{i+1/2,j}^{n} + \frac{\Delta t}{12}\left[23F_{i+\frac{1}{2},j}^{n} - 16F_{i+\frac{1}{2},j}^{n-1} + 5F_{i+\frac{1}{2},j}^{n-2}\right] \tag{12}$$

$\eta_{i,j}^{n+1}$ is obtained directly but the velocity in the future time step $U_{i+1/2,j}^{n+1}$ is calculated by solving a matrix system. Calculated values of u and η are utilized in the corrector step and in doing so, the correct values of these parameters are obtained. In the corrector step, equations 5 and 6 are used through the fourth-order Adams-Moulton method.

$$\eta_{i,j}^{n+1} = \eta_{i,j}^{n} + \frac{\Delta t}{24}[9E_{i,j}^{n+1} + 19E_{i,j}^{n} - 5E_{i,j}^{n-1} + E_{i,j}^{n-2}] \tag{13}$$

$$U_{i+\frac{1}{2},j}^{n+1} = U_{i+\frac{1}{2},j}^{n} + \frac{\Delta t}{24}\left[9F_{i+\frac{1}{2},j}^{n+1} + 19F_{i+\frac{1}{2},j}^{n} - 5F_{i+\frac{1}{2},j}^{n-1} + F_{i+\frac{1}{2},j}^{n-2}\right] \quad (14)$$

The predictor-corrector process continues until the error between two sequential results reaches an acceptable limit. The error is obtained for any variable by the equation

$$\Delta f = \frac{\sum_{i,j}|f_{i,j}^{n+1} - f_{i,j}^{(n+1)^p}|}{\sum_{i,j}|f_{i,j}^{n+1}|} \quad (15)$$

where f can be η or u and $(\ )^p$ denotes the previously found values of the variables. Here, the predictor-corrector procedure is stopped when $\Delta f < 0.0001$. To ensure the stability of the numerical scheme, the Courant number (*Cr*) is considered as a criterion. Lin and Man (2007) used the stability analysis due to von Neumann for Nwogu's Boussinesq equations. In their analysis, predictor and corrector steps have been analyzed separately and it has been shown that the method is stable when *Cr* is less than or equal 1 for the predictor step and 0.5 for the corrector step. *Cr* value is calculated as follows

$$Cr = \sqrt{gh}\left(\frac{\Delta t}{\Delta x}\right) \quad (16)$$

We use relation (16) satisfying time and spatial variations in the construction of the mesh size.

3.2 Boundary conditions

For any numerical model, implementing proper boundary conditions is essential in order to obtain accurate results. In our study, two types of boundary conditions are considered: the fully reflective boundary (solid wall) and the absorbing boundary (sponge layer). These boundary conditions are discussed in the following sub-sections.

3.2.1 Fully reflective boundary (solid wall)

Waves are completely reflected when colliding with solid walls and almost no energy is absorbed by the wall. If n represents the unit normal vector then the velocity and surface elevation relation for this boundary is as follows

$$u.n = 0 \quad or \quad u.n_x = 0 \ \rightarrow \quad u = 0 \quad (17)$$

$$\nabla\eta.n = 0 \quad or \quad \nabla\eta.n_x = 0 \ \rightarrow \quad \nabla\eta = 0 \quad (18)$$

Fig. 1 displays the schematic of a solid wall for the right side of the domain. The present numerical model requires three ghost cells after the wall, because of the high order estimation of the spatial derivatives. Ghost cells values are described as

$$\eta_{i+2} = \eta_{i+1} \quad , \quad \eta_{i+3} = \eta_I \quad , \quad \eta_{i+4} = \eta_{i-1} \quad (19)$$

$$u_{i+5/2} = u_{i+1/2} \quad , \quad u_{i+7/2} = u_{i-1/2} \quad (20)$$

and the velocity on the boundary is defined as $u_{i+3/2} = 0$.

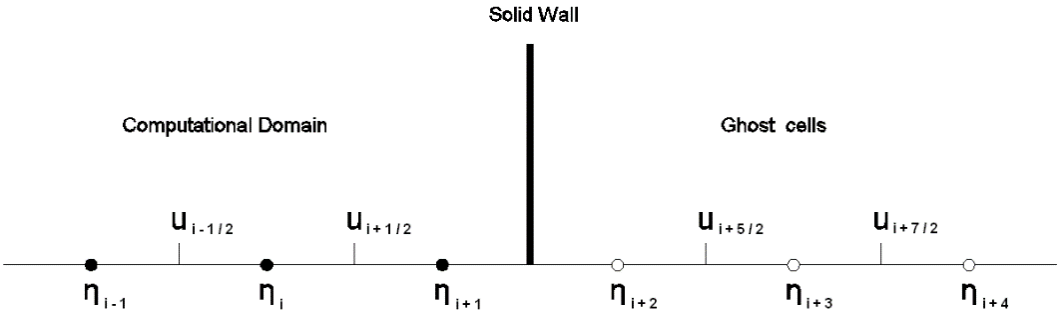

Fig. 1 Staggered-grid system on the solid wall where waves are fully reflected. Points of ghost cells are used to help discretize spatial derivatives at the endpoints of the computational domain

3.2.2 Absorbing boundary (sponge layer)

Wave absorption in external boundaries is highly important to avoid any reflection. The energy of waves entering such a non-reflecting boundary has to be absorbed by the end of the channel in order to properly simulate the free field wave propagation. A full sponge layer absorbs all the energy and prevents the waves from reflecting the domain. In the sponge layer boundary condition, to absorb the energy of the wave, the water surface elevation, and wave horizontal velocity are multiplied by a coefficient function C after each time step, where C is defined as (Tonelli and Petti 2009)

$$C\ (x) = \begin{cases} 0.5 + 0.5\,cos\left(\pi \frac{Ws - Ds(x)}{Ws}\right) & Ds \le Ws \\ 1 & Ds > Ws \end{cases} \tag{21}$$

Here Ws is the width of the sponge layer taken to be 4 m in our tests and Ds is the distance between the point and the beginning of the sponge layer. For better performance of a sponge layer, the layer width should be at least as long as the wavelength.

In the next section, we demonstrate the implementation of our numerical model described above for solving (3) and (4) for a variety of test cases using the solid wall and spongy boundary conditions. We first validate our scheme with flat planar and sloping (variable and running) obstacles in the presence of a solitary wave and then discuss wave interactions with semicircular and rectangular breakwaters.

3.2.2 Incident wave boundary

Since the discovery of the existence of solitary waves by Russell (1884), many researchers started finding properties of the solitary waves via theoretical studies and documented very valuable results. Because of the simple nature of the solitary wave equations, as compared to other wave equations, solitary wave theory is frequently employed in various investigations of near beach waves.

4. Validation tests

In order to assess the capability of the model in simulating waves, various tests have been taken into consideration. The objectives of these tests are to validate our numerical model and to assess the nonlinear and dispersion terms in the governing equations. To achieve this goal we consider five tests as described in the following sub-sections. In all tests, the ratio of the wave height to water depth H/h is less than 0.77, which is smaller than the critical breaking index value (McCowan 1894 and Miche 1944).

Two types of solitary waves for extended Boussinesq model equations that are of interest in the present context are as follows. The first one used for water surface elevation in the work of Tonelli and Petti (2009) is

$$\eta(x,t) = H.sech^2[\sqrt{\frac{3H}{4h^3}}(x-ct)] \tag{22}$$

where H is the solitary wave height and $C = \sqrt{g(H+h)}$ is the wave velocity. By using low order approximation, the horizontal depth-averaged velocity in this case is

$$u = \frac{\sqrt{gh}}{h}\eta \tag{23}$$

Another the solitary-wave solution for Nwogu's model equations proposed by Wei and Kirby (1995) for the surface elevation η and horizontal velocity u of solitary wave are

$$\eta(x,t) = A_1.sech^2[B(x-ct)] + A_2.sech^4[B(x-ct)] \tag{24}$$

$$u = A.sech^2[B(x-ct)] \tag{25}$$

where A, A_1, A_2, and B are defined in appendix I of Wei and Kirby (1995) study. It should be mentioned that we used both the solitary wave types and found that they produce numerically identical results as shown later in Figures 7 and 11. Therefore, we used the simplified solitary wave solution (22) and (24) in our computations and simulations.

4.1 Test 1: Solitary wave propagation over flat bottom

Propagation of a solitary wave in a long distance is a standard test utilized by numerous authors (e.g., Shiah and Mingham 2009, Wei and Kirby 1995). This test analyzes the conservative and stability properties of the numerical scheme. By modeling the solitary wave propagation over a constant depth, Tonelli and Petti (2009) tested their hybrid finite volume-finite difference scheme for solving the 2DH improved Boussinesq equations and Li *et al.* (1999) also validated their finite element method (FEM) that is used for solving their improved Boussinesq equations.

In the current study, solitary wave propagation at a constant depth $h = 0.5\ m$ is simulated in a channel of length $Lc = 300\ m$. Grid size is $\Delta x = 0.1m$ and the time step is set to be $\Delta t = 0.01\ s$. The considered solitary wave with height $H = 0.05\ m$ propagates for $100\ s$ from the location $x = 50\ m$. We implemented our numerical scheme and ran the simulation for a long time for comparison with an analytical solution. The results are discussed in subsection 6.1.

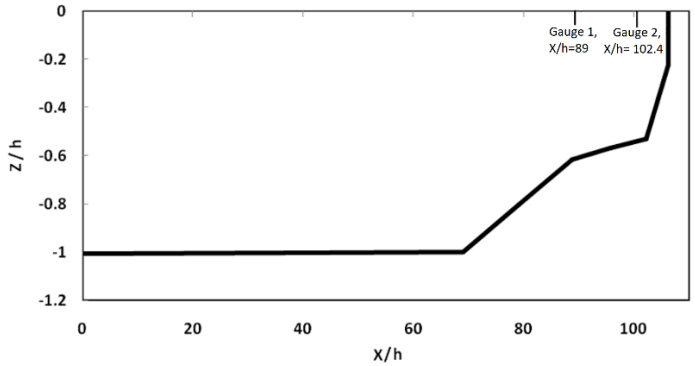

Fig. 2 Diagram illustrating numerical channel with variable slopes. The wave generated at the left part of the channel runs up the slope and returns after colliding with the solid wall located at the right

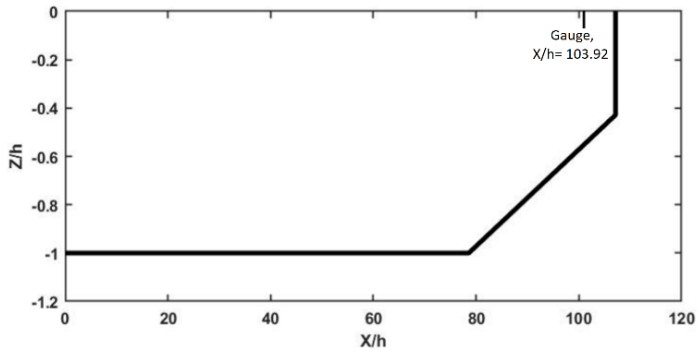

Fig. 3 Schematic of the numerical channel of 1:50 slope. The wave generated at the left part of the channel runs up the slope and returns after colliding with the solid wall located at the right end

4.2 Test 2: Solitary wave propagation over variable slopes

Solitary wave run-up over shore slopes is used as a good test to analyze the nonlinear effects of the model (e.g., Ghadimi and Lamouki 2017, Wei *et al*. 1995). Since wave height increases with decreasing water depth, the effects of nonlinear terms near beaches become more significant. For this reason, a channel with length *Lc* = 106.5h as shown in Fig. 2, is modeled. In this simulation, the channel is divided into 1065 segments and the time step is set to be $\Delta t = 0.01\ s$. The channel depth ($h = 0.218\ m$) is constant up to $x/h = 68.99$ and after that, the beach extends in three stages with three slopes 1:53 (length 20 h), 1:150 (length 13.44 h) and 1:13 (length 4.13 h). Dimensionless wave height of the solitary wave at the starting point is $(\frac{H}{h}) = 0.2602$. Two gauges are placed in the channel to measure the water surface elevation height. Gauges 1 and 2 are located at $x/h = 89$ and $x/h = 102.43$, respectively. Our numerical findings are compared with the available experimental results (see subsection 6.2).

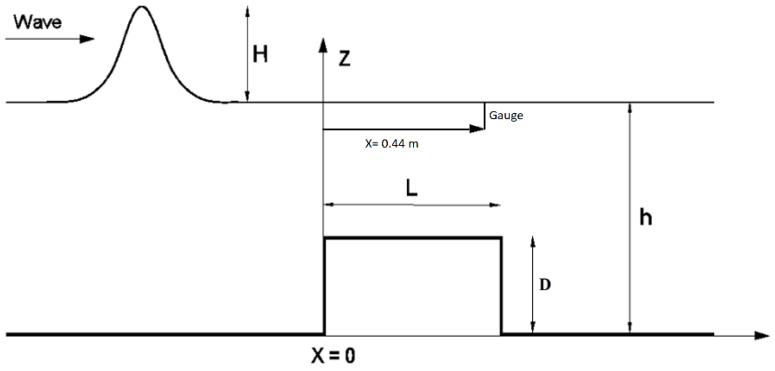

Fig. 4 Computational domain of the solitary wave propagation over a rectangular submerged breakwater. The wave generated at the left part of the channel propagates over the channel length and passes the breakwater. Two gauges are located at the left ($x = -8.2\ m$) and the right side ($x = 0.44\ m$) of the coordinate center (left face of the cross-section of the breakwater) to extract time history of the solitary wave surface elevation

4.3 Test 3: Wave reflection after the running up the slope

In the present case, after running up a beach slope, a solitary wave collides with a solid wall and gets reflected. The test is suitable for analyzing the nonlinear terms of the model and the reflection boundary condition. The test also allows the model for analyzing propagation velocity in the presence of reflection which is a highly influencing parameter on the velocity. A representation of the domain is depicted in Fig. 3 and is similar to those used by Walkley (1999) and Dodd (1997). Domain length is *Lc* = 75h m and the solitary wave center at the starting moment is $x/h = 35.71$. At first, the wave propagates over a constant depth ($h = 0.7\ m$) and then reaches a slope at point $x/h = 78.57$. At the end of the 1:50 slope, the wave collides with a solid wall, reflects, and returns to the domain. The time step and grid lengths are $\Delta t = 0.01\ s$ and $\Delta x = 0.1\ m$, respectively. The solitary wave of height $H = 0.07\ m$ propagates for a total time of 30 s along the channel. To extract the time history of wave surface elevation, the gauge is placed at point $x/h = 103.92$. A comparison of our results with the experimental data is provided in subsection 6.3.

4.4 Test 4: Solitary wave propagation over a rectangular submerged breakwater

To reduce the energy and height of the incoming waves towards the shore, a marine structure is usually installed near the shoreline. Due to these practical applications, the solitary wave propagation over marine structures has been the subject of many numerical and experimental studies (Cheng and Hsu 2013, and Liu *et al*. 2011). The results of such investigations play a significant role in several marine engineering tasks. The Solitary wave is frequently applied for modeling the nonlinear long waves including tsunami waves (Murashige and Wu 2010). Furthermore, the analysis is commonly used to calculate the RTD coefficients of submerged breakwaters (Lynett *et al*. 2000). Lin (1998) analyzed the interaction between the solitary wave with the rectangular obstacles numerically and computed the RTD coefficients by assuming variations in the submerged breakwater height and width.

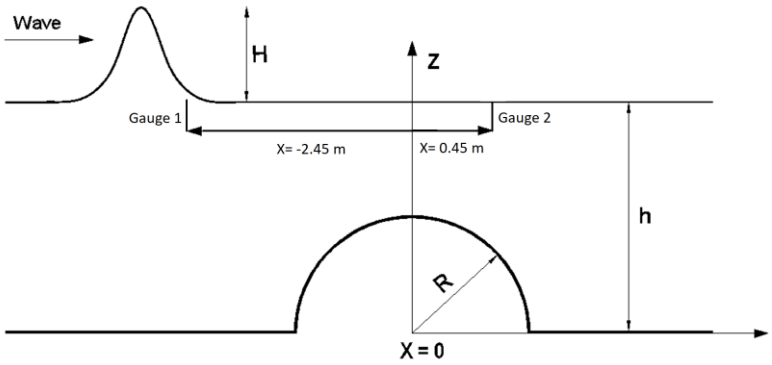

Fig. 5 Computational domain of the solitary wave propagation over a semicircular submerged breakwater. The wave generated at the left part of the channel propagates over the channel length and passes the breakwater. Two gauges are located at the left (Gauge 1, $x = -\ 2.45\ m$) and the right side (Gauge 2, $x = 0.45\ m$) of the coordinate center (center of the semicircle) to extract the time history of the solitary wave surface elevation

Using this test, the capability of the model to simulate the interaction between solitary waves and rectangular submerged breakwaters is analyzed. The schematic of its domain is illustrated in Figure 4. The breakwater starts at $x = 0$. A sponge layer is applied at the end of the channel to absorb the wave and to prevent its reflection. The submerged breakwater length is $L = \ 0.4\ m$ and its height is $D\ = 0.08\ m$. The solitary wave with height $H\ =\ 0.0288\ m$ propagates over the channel with depth h = 0.16 m and the time step is $\Delta t = 0.005\ s$ and grid length is $\Delta t = 0.05\ m$. The gauges have been located at two sides of the submerged breakwater in order to show the changes in wave height as a result of passing over the breakwater. Gauge number 1 is situated at x = -8.2 m and gauge number 2 at x = 0.44 m. Our computed results are compared with the experimental findings (see subsection 6.4).

4.5. Test 5: Propagation of solitary wave over the semicircular submerged breakwater

The first investigation on semicircular submerged breakwaters appears to have been conducted in Miyazaki port in 1993 as reported by Cheng & Zheng (2003). The application of the breakwaters of this configuration has been growing because of good stability and low cost. Young and Testik (2011, 2009) later studied the interaction between waves and semicircular submerged breakwaters experimentally.

To display the capability of our numerical model to simulate semicircular submerged breakwaters, the following test has been considered. As shown in Fig. 5, the center of the circular section with radius $R = 0.6\ m$ is located at $x = 0$. The Solitary wave with height $H = 0.311\ m$ propagates over a channel of depth $h = 1\ m$. Gauges at $x\ =\ -\ 2.45\ m$ (gauge 1) and $x\ =\ 0.45\ m$ (gauge 2) have been considered at two ends of the submerged breakwater to measure the water surface elevation. The time step and grid length in this test are $\Delta t = 0.005\ s$ and $\Delta x = 0.05\ m,$ respectively. In subsection 6.5 the numerical results are compared with the available experimental data.

Table 1 Dimensions of the considered semicircular and rectangular submerged breakwaters. R is the radius of the semicircular breakwater. D and L are the height and length of the rectangular breakwater, respectively

Dimensions of submerged breakwaters (m)										
Semicircular	R	0.5	0.45	0.4	0.35	0.3	0.25	0.2	0.15	0.1
Rectangular	D	0.5	0.45	0.4	0.35	0.3	0.25	0.2	0.15	0.1
	L	0.393	0.353	0.314	0.275	0.236	0.196	0.157	0.118	0.079

5. New comparison set up for semicircular and rectangular submerged breakwaters

As mentioned in the introduction and in the preceding section, the studies for wave interactions with obstacles of semicircular and rectangular shapes have been performed in a variety of contexts. However, a systematic comparison of data suggesting a specific choice has not been provided so far. In this section, we provide a set up for implementing our numerical scheme to compare performances of semicircular and rectangular submerged breakwaters that are determined and compared via the RTD coefficients.

5.1.1 Numerical model implementation

The behavior of breakwaters of various shapes interacting with waves is a key factor to determine a suitable choice. The RTD coefficients for submerged breakwaters provide knowledge on such behavior when interacting with waves. By studying these coefficients, a better choice of the geometry for submerged breakwaters could be determined. The costs of building submerged breakwaters with the least amount of material to get the highest performance is another necessary factor. Previous numerical studies focused on individual types of the submerged breakwater and determined RTD coefficients (see, Lin 2004, Young and Testik 2009, 2011, for instance). In this study, we analyze and compare the performance of the rectangular and semicircular submerged breakwaters, when interacting with solitary waves.

For comparison of the rectangular and semicircular obstacles interacting with waves, a channel with length $Lc = 310\ m$ and depth $h = 1\ m$ is considered. The rectangular and semicircular submerged breakwaters are located at the final 45 meters on the right side of the channel. The solitary wave is set to move from the left side of the channel at $x = 10\ m$. For a better comparison, various height from $H = 0.1\ m$ to $0.5\ m$ have been considered for the solitary wave. In the present study, for each radius of the semicircular breakwater, a rectangular submerged breakwater with a crest height (d) equal to the circular radius (R) is considered which varies between $0.1\ m$ to $0.5\ m$.

The length (L) of the rectangular section is taken in such a way that its area equals the area of the related semicircular section (That is, $\mathrm{D} * \mathrm{L} = \frac{\pi \mathrm{R}^2}{2}$). The related dimensions of each breakwater are given in Table 1. We return to analyze the performance of submerged breakwaters with the equal area and crest height while varying their crest width and length later.

5.1.2 Determination of the RTD coefficients

Wave energy is absorbed by various means when colliding with marine structures and natural obstacles. After the collision, part of the wave energy gets reflected, a portion of it passes through the structure and the remaining part is damped due to reflection and the friction at the bottom. In order to display the effects of marine structures on waves, coefficients of reflection (K_R), transmission (K_T) and dissipation (K_D) are used and are calculated via the relations given below.

If the reflection and transmission coefficients themselves are energy conserved then the diffusion coefficient does not arise. Note that the reflection coefficient (K_R) is the ratio of the reflected wave height (H_r) to the incident wave height (H_i) and the transmission coefficient (K_T) is the ratio of the transmitted wave height (H_t) over the breakwater to incident wave height (Lin 2004, Lin and Karunarathna 2007). The relationships among these coefficients are

$$K_R = (\frac{H_r}{H_i}) \tag{26}$$

$$K_T = (\frac{H_t}{H_i}) \tag{27}$$

Our numerical results indicate that the wave interactions with breakwater structures generate non-energy conserved K_R and K_T. This, in turn, yields a dissipative type of contribution K_D (Dissipation coefficient) which is defined as

$$K_D = \sqrt{1 - (K_R)^2 - (K_T)^2} \tag{28}$$

Observe that with these relations the three RTD coefficients satisfy (the energy conservation)

$$K_R^2 + K_T^2 + K_D^2 = 1 \tag{29}$$

In all our numerical models, the H_t is measured 2 m from the right edge of the breakwater while H_r, and H_i are measured 2 m and 5 m from the left edge of the breakwaters, respectively (see Figs. 4 and 5).

6. Computational results

In this section, the computational results of the proposed numerical model are presented and compared against existing analytical, experimental and numerical data. First, the results for various tests involving topographical obstacles discussed in the previous section are illustrated and validated. The numerical comparative study of the performances of the semicircular and rectangular breakwaters while interacting with solitary waves is then documented.

6.1 Solitary wave propagation over flat bottom

The computed results for the wave propagation with a flat bottom topography based on our numerical scheme are compared with the analytical solution andnumerical modeling (Wei and Kirby 1995) and displayed in Fig. 6. Fig. 6 shows the wave travelling for t = 100 s. While the wave height remains constant for a long distance and for a longer simulation time, there is a slight decrease of about 1.66 percent is noticed in the wave height. There is also a small phase change relative to the

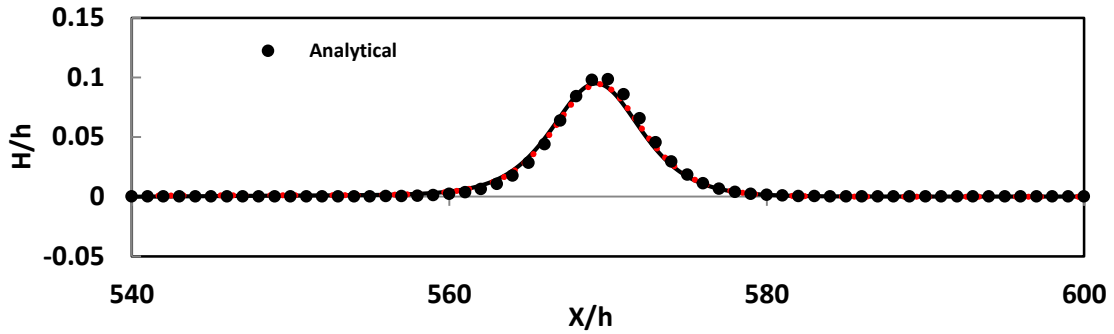

Fig. 6 Comparison of the numerical and analytical solitary wave profiles after propagating for 100 seconds. The starting point of the wave movement is at $x = 50\ m$ and the height of the wave is $H = 0.05\ m$

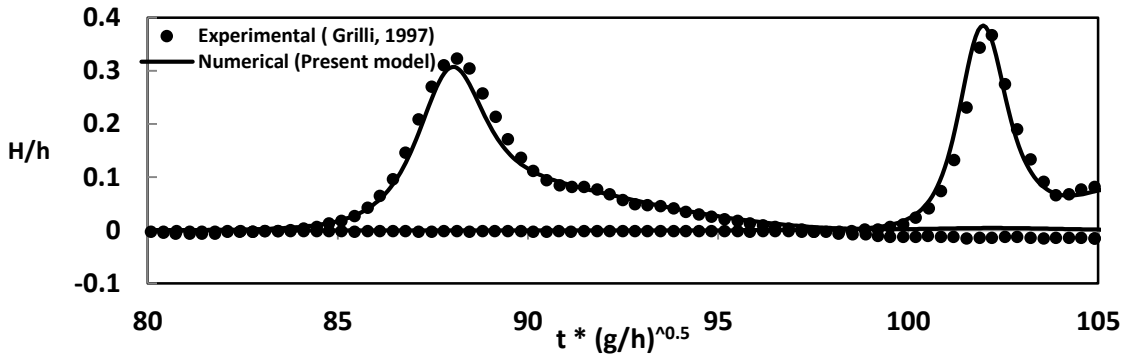

Fig. 7 Time history of the numerical and experimental solitary wave surface elevations for $H/h = 0.2602$. Two gauges are located at $x/h = 89$ (Gauge 1, first peak) and $x/h = 102.43$ (Gauge 2, second peak) to obtain the time history

analytical wave. Thus, the long-distance comparison reveals small changes in the wave height in comparison to the analytical results, however, Is shows a good match with numerical modelling (Wei and Kirby 1995).

6.2 Solitary wave propagation over variable slopes

In Fig. 7, the time history of the numerical results for wave propagation over variable slop has been compared against the experimental results obtained by U.S. Army Engineering Waterways Experiment Station (Grilli 1997). As portrayed in this figure, water surface elevation at gauge 1 has a good overlap on the experimental results. At gauge 2, there is a slight time lag between experimental and numerical results. Also, numerical wave height at gauge 1, unlike gauge 2, is less than the experimental wave height which is due to the increased effects of the nonlinear terms. As the wave approaches the breaking zone, numerical model wave height increases, as expected. It is observed from our results that there is a reasonable 4.94 percent error in the obtained wave height.

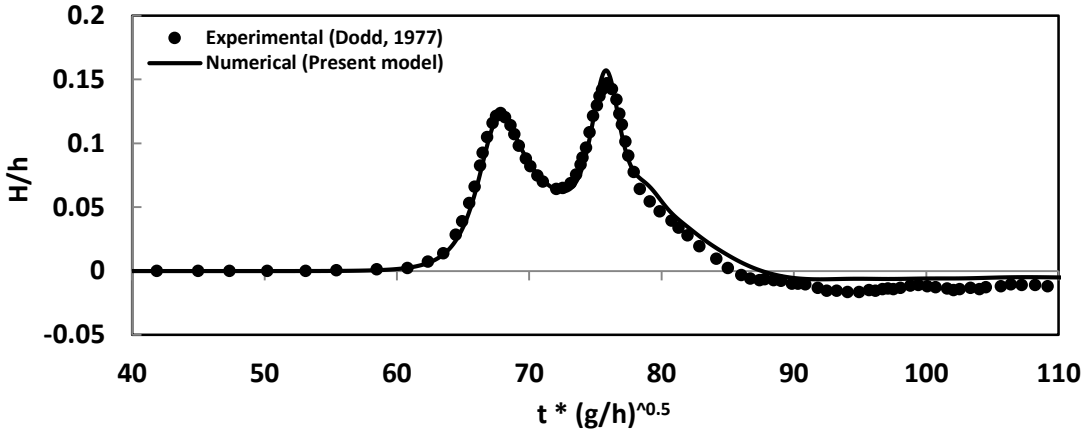

Fig. 8 Time history of the numerical and experimental solitary wave surface elevations at $x/h = 103.92$. The first peak (located at the left part of the diagram) and the second peak (located at the right part of the diagram) show the time history of the wave before and after colliding with the solid wall, respectively

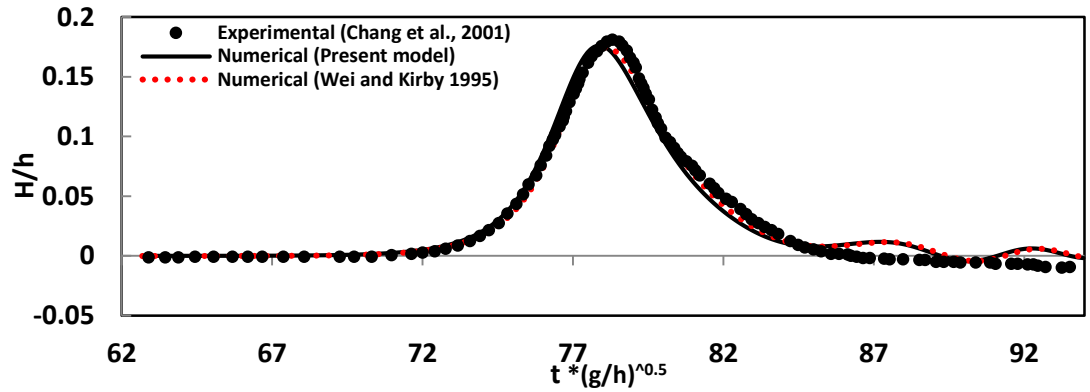

Fig. 9 Time history of the numerical and experimental solitary wave surface elevations at $x = 0.44\ m$. The height of the solitary wave is $H = 0.0288\ m$

Relative low differences between numerical and experimental results reveal that the model is capable of simulating wave run-up at the beach with variable slopes together with nonlinear effects.

6.3 Wave reflection after running up the slope

The numerical results for this case are compared with the experimental data provided by Dodd (1997) as shown in Figure 8. The first peak is related to the incoming wave and the second peak is associated with the reflected wave. As displayed in Fig. 8, for the incoming wave elevation simulated with high precision, the reflected wave has a slight increase of 7.09 percent in height relative to the experimental results. However, the results are still in good agreement with the experimental data, and the presence of nonlinear terms with a fully reflective boundary condition is well simulated.

6.4 Solitary wave propagation over a rectangular submerged breakwater

To validate our numerical model for the solitary wave interaction with a rectangular submerged breakwater, we compared our results with the experimental data by Chang *et al*. (2001) and numerical modeling by Wei and Kirby, (1995), and the graphical illustration is provided in Fig. 9. After the wave passes over the submerged breakwater, a slight deformation of the wave profile arises due to the effects of reflection and dispersion as shown in Fig. 9. We remark that the dispersion effects with turbulence can also be precisely modeled in an analogous fashion. The wave height obtained by the model has a deviation of 4.09 percent from the experimental results. Also, there exists a wave train after the observation of the main wave which is a result of the wave hitting with the barrier. This shows that there is a consistency between the results of the numerical model and experimental data is acceptable and therefore it is safe to say that our numerical model is suitable in simulating the interaction between solitary waves and rectangular submerged barriers.

6.5 Interaction of solitary wave with the semicircular submerged breakwater

Computed wave heights using the proposed numerical model are compared with the experimental results (Cooker et al., 1990) and numerical results (Jabbari *et al*. 2013) in Fig. 10. As observed in this figure, the water elevation is well simulated compared with the experimental results using the numerical model due to Jabbari *et al*. (2013) and our present computational scheme. As displayed in Fig. 10, at gauge 1 (x= -2.45 m), a slight difference is observed. The difference increases by passing over the breakwater and the increase is about 1.84 percent. This could be partially due to the dispersion effects and the increasing effects of the nonlinear terms. Further, since the equations are solved by the use of finite difference technique, the approximation related to bottom slope tends to be infinite at the start and the end of the semicircular submerged breakwater resulting in additional changes in the wave profile.

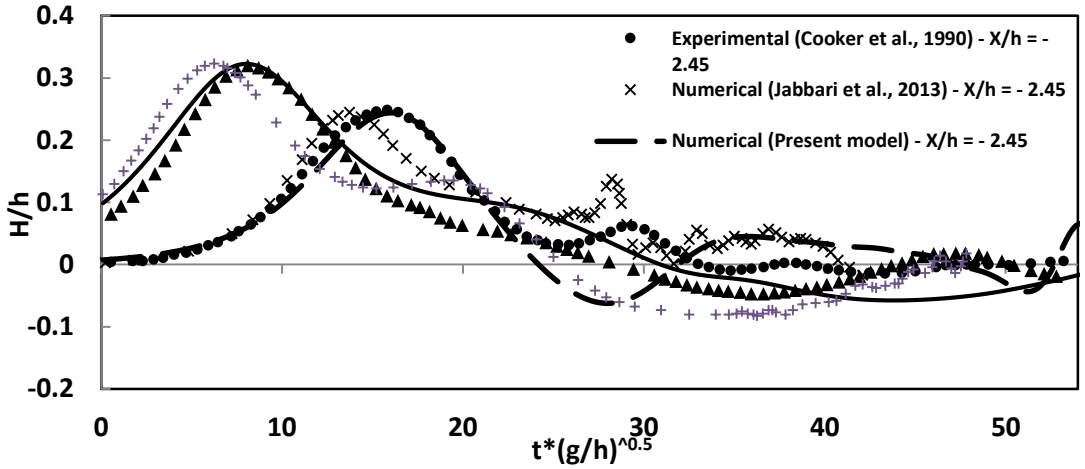

Fig. 10 Time history of the water surface elevations at $x = -2.45\ m$ (Gauge 1) and $x = 0.45\ m$ (Gauge 2). The height of the solitary wave is $H = 0.311\ m$

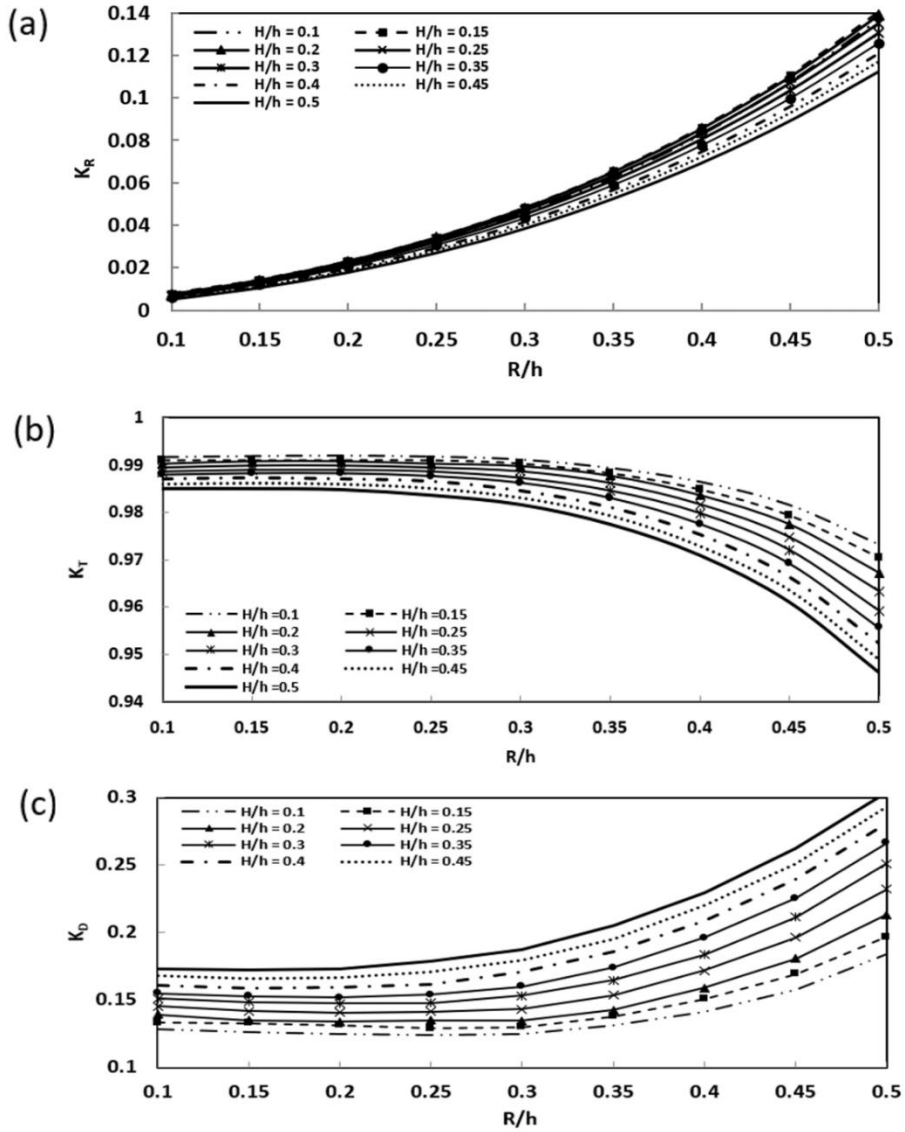

Fig. 11 Distribution of RTD coefficients for the semicircular sections. The range of wave heights and breakwater heights is 0.1 – 0.5 *m*. Diagrams a, b, and c illustrate the reflection coefficient, transmission coefficient, and dissipation coefficient, respectively

6.6 RTD coefficients for semicircular and rectangular barriers

The numerical values of the reflected and transmitted wave heights have been obtained at a distance $15\ m$ from the submerged breakwater center. The RTD coefficients related to various semicircular and rectangular breakwaters are illustrated in Figs. 11 and 12. As mentioned earlier, the

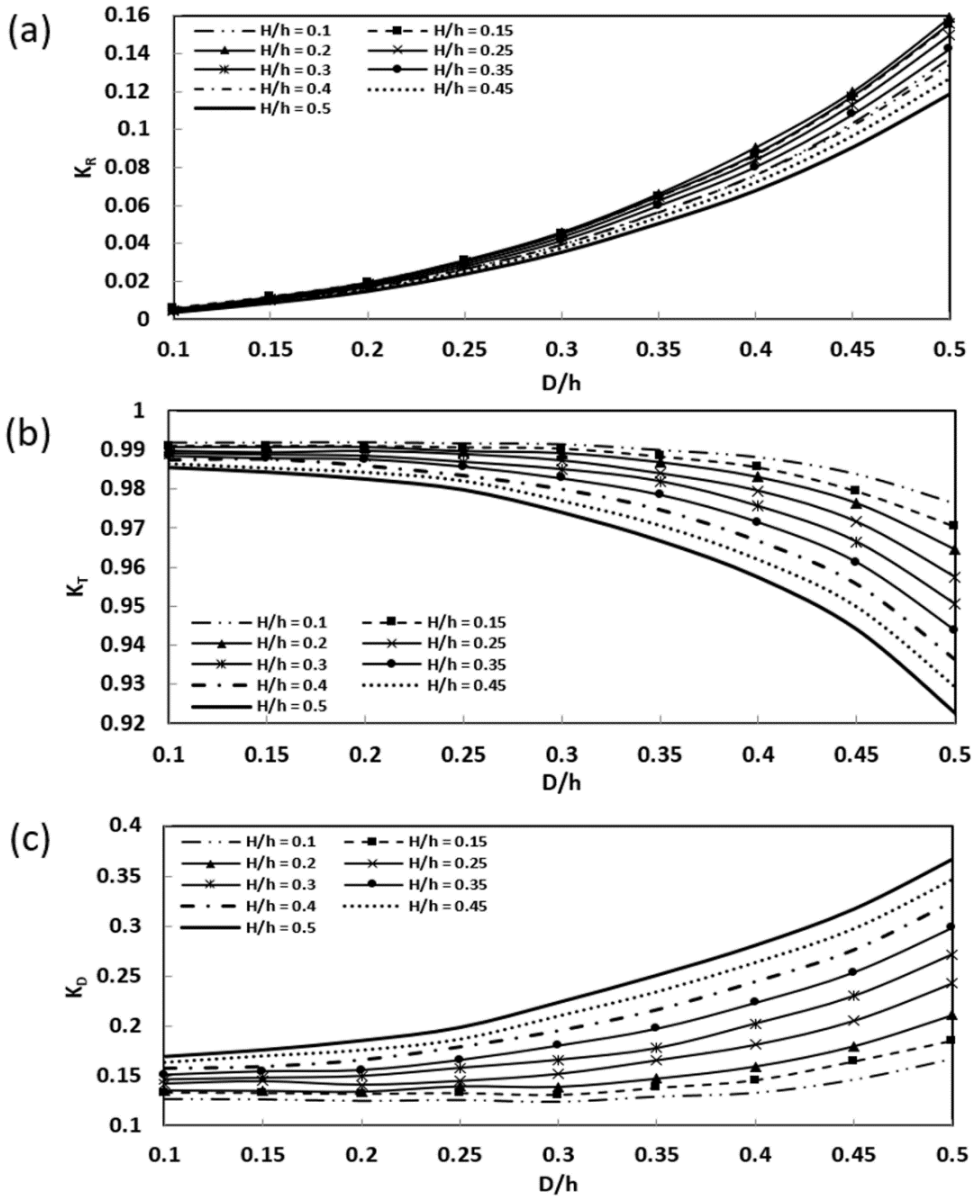

Fig. 12 Distribution of RTD coefficients for the rectangular sections. The range of wave heights and breakwater heights is 0.1 – 0.5 *m*. Diagrams a, b, and c illustrate the reflection coefficient, transmission coefficient, and dissipation coefficient, respectively

reflection and transmission coefficients do not yield conservation of energy due to strong interactions between the wave and the semicircular and rectangular barriers. The difference produces dissipative type of effect and makes the energy conserved according to (Eq. (29)).

It is observed that, as the submerged breakwater crest height increases, the reflection coefficient gradually increases for both semicircular and rectangular configurations and the corresponding variation between them ranges from 0.00 to 0.16 (Figs. 11(a) and 12(a)). In contrast, as the height of obstacles rises, the transmission coefficient decreases. Its variation ranges from 0.92 to 1.00 as seen in Figs. 11(b) and 12(b), respectively. As expected, changes in the reflection and transmission coefficients have different trends. The reason is that as the height of breakwater increases, a bigger part of the wave is reflected by the breakwater and therefore, a smaller part of the wave passes over it. A lower K_T indicates that the wave is better damped by a higher breakwater. Figs. 11(c) and 12(c) confirm these statements as well. The dissipation coefficient variation ranges from 0.10 to 0.35. These illustrations can easily be adapted for the engineering design of the rectangular and semicircular breakwaters. Furthermore, with the help of these curves, the RTD coefficients related to obstacles with different height and lengths in the desired ranges can be easily and reliably determined.

6.7 Comparison of the performances of the semicircular and rectangular submerged breakwaters

The best method for comparing the performances of semicircular and rectangular submerged breakwaters is through their RTD coefficients. To this end, the reflection coefficients of the two submerged breakwaters are compared in Fig. 13(a). As observed in this figure, each curve is related to a submerged breakwater of constant crest height and shows K_R in different wave heights. The results indicate that with increasing the height of breakwaters, the difference in the K_R coefficient between the two structures increases as evident from Fig. 13(a).

A comparison of the transmission coefficients for semicircular and rectangular breakwaters is illustrated in Fig. 13(b). As pointed out earlier, bigger reflected waves result in smaller transmitted waves leading to lower transmission coefficients. Hence, breakwaters with height 0.5 m that have the highest reflected coefficient have the lowest transmission coefficient.

Next, the dissipation coefficients related to the submerged breakwaters are depicted in Fig. 13(c). It can be seen from this figure that increased wave height results in higher dissipation coefficients. The results of three RTD coefficients show that the dissipation coefficients has a direct and inverse relation with the reflected and transmission coefficients, respectively.

7. Discussion of the numerical results

Analysis of the RTD coefficients of the breakwaters can furnish a better understanding of the performances of the structures used. For this reason, RTD coefficients of semicircular and rectangular breakwaters are discussed and analyzed in this section.

7.1. K_R coefficient

In the case of semicircular and rectangular submerged breakwaters of low heights, a lower reflection coefficient is achieved and both sections perform similarly. This similarity can be observed in Figure 13a in the case of submerged breakwaters of the height of $0.1\ m$. In this breakwater height range, wave height does not affect the reflection coefficient as seen in this figure.

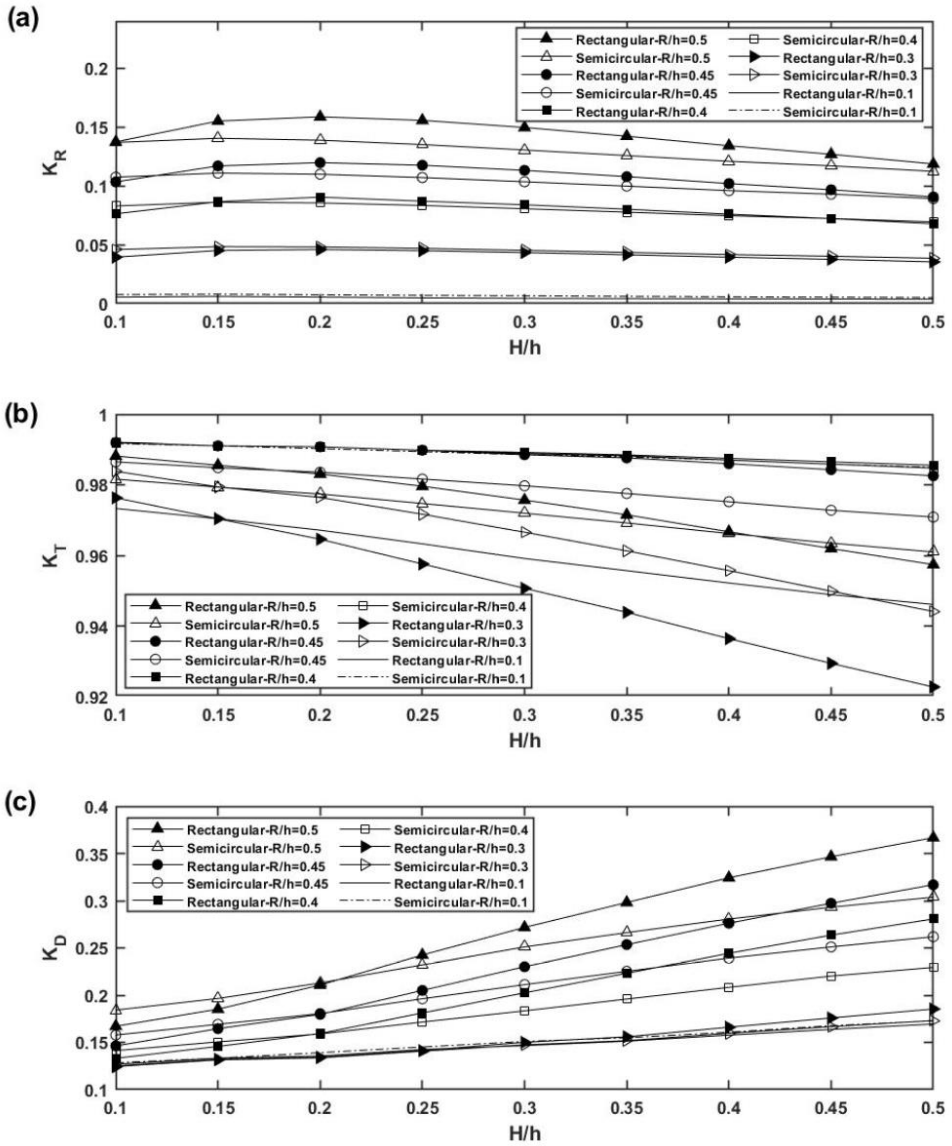

Fig. 13 (a) Comparison of the reflection coefficients of the semicircular and rectangular sections for different H/h and R/h or D/h. (b) Comparison of the transmission coefficients of the semicircular and rectangular sections for different H/h and R/h or D/h. (c) Comparison of the dissipation coefficients of the semicircular and rectangular sections for different H/h and R/h or D/h

As the height of the submerged breakwater rises, higher reflection coefficients are obtained. Increase in breakwater height not only affects the K_R coefficients of both geometries but also the difference between them. In these cases, rectangular submerged breakwaters perform better than semicircular breakwaters and achieve higher reflection coefficients. As wave height increases, the difference in K_R coefficient between the two types of submerged breakwater decreases which are easily observed in breakwater with a height of $0.5\ m$ (Fig. 14(a)). In this crest height range, for high ($H/h > 0.4$) and small ($H/h < 0.15$) waves, the reflection coefficients of the semicircular and rectangular sections approach each other. The similarity in the performance of the two sections may be interpreted as follows. Since the height of the submerged breakwaters is lower, consequently the effect of geometry becomes smaller. By increasing the wave height, K_R becomes more and more sensitive to the geometrical shape of the breakwater. However, as the ratio H/h increases further (for example $H/h = 0.45$ to R/h or $D/h = 0.5$), it is observed that K_R coefficients in the two types of submerged breakwaters approach each other again which indicates that geometry in the case of a high wave does not significantly affect the reflection performance of the breakwater.

For a better interpretation of the performance of the two breakwaters, the reflection coefficients of the circular breakwaters are subtracted from that of the rectangular breakwaters and the normalized coefficients are shown in Figure 14a. This graph creates an opportunity to compare the reflection performance of the two breakwaters at a glance. It is found that the rectangular submerged breakwater with ratios $D/h >= 0.45$ and $0.15 < H/h < 0.45$ has performed 5-15% better relative to semicircular submerged breakwater. In the ranges other than the one mentioned here, submerged breakwater shape has a less significant influence on the reflected wave height.

7.2 K_T coefficients

For lower values of breakwater height (e.g. R or $D = 0.1\ m$), due to weak effects of the submerged breakwater on waves, higher values of K_T are obtained using our numerical scheme as shown in Fig. 13(b). This, in turn, implies that the waves pass over the breakwaters with no distinctive effect due to the height of the barrier. The performance of both geometry shapes is similar to each other in this specific range. However, it is observed that, as the crest height of submerged breakwater increases, the breakwater shape affects the transmission coefficient significantly. In higher submerged breakwaters situations (R/h or $D/h > 0.2$), as wave height rises, the difference between transmission coefficients of rectangular and semicircular breakwaters increases and rectangular submerged breakwater achieves lower K_T values relative to the semicircular submerged breakwater. The most decrease in the amount of K_T happens for the rectangular breakwater with a crest height of $D = 0.5\ m$ and wave height of $H = 0.5\ m$. In this case, the performance is about 2.47 percent better (due to lower K_T) compared to the semicircular breakwater of the same characteristics (Fig. 14(b)). One reason behind this fact is that the rectangular section has a relatively longer crest.

7.3 K_D coefficients

In the interaction of waves and submerged breakwaters with low crest height, the dissipation coefficient is low, but increasing the submerged breakwater crest height causes the dissipation coefficient to rise. Fig. 14© clearly shows the effects of the geometry of the submerged breakwater on the dissipation. It is observed that rectangular submerged breakwater results in a better dissipation for higher waves, it has about 3-23% better dissipation performance than the semicircular submerged

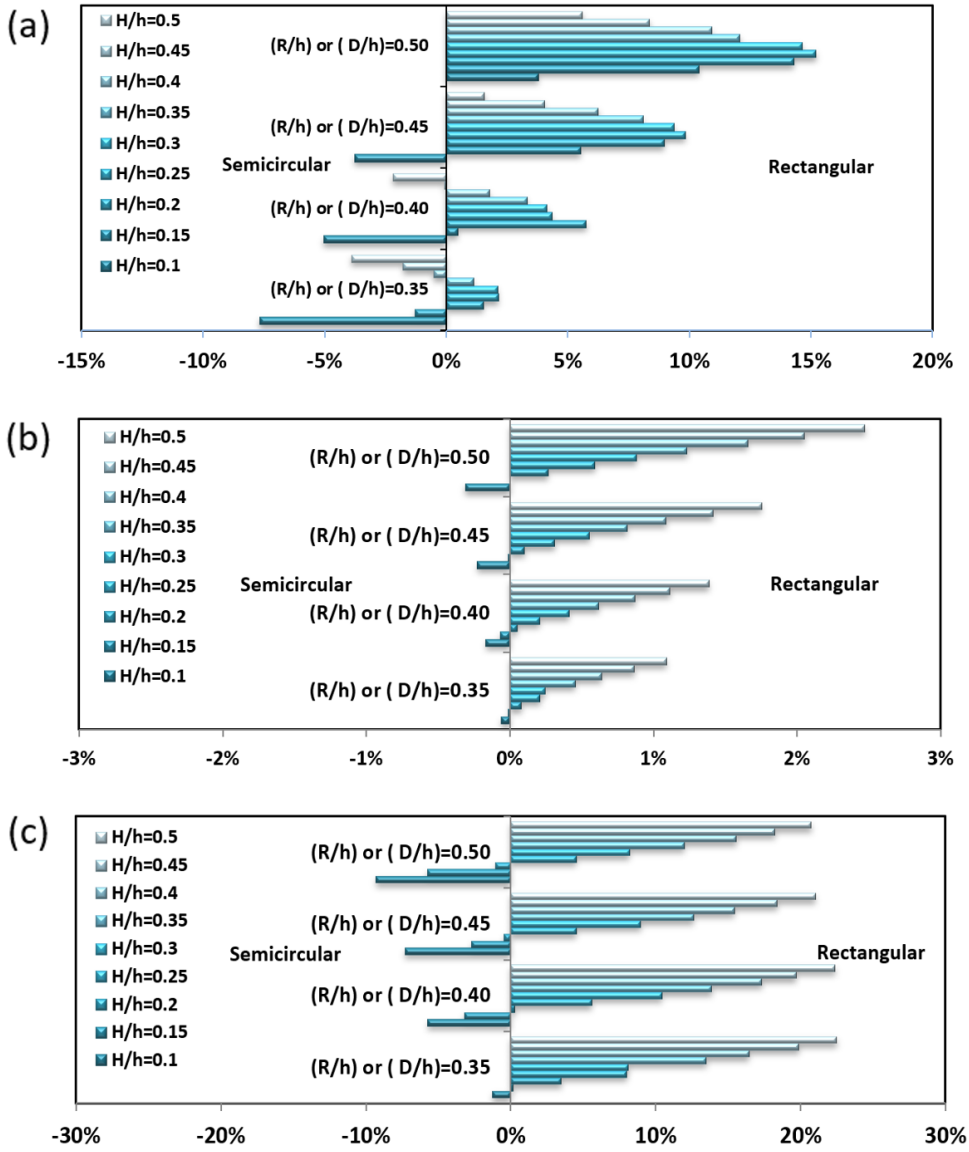

Fig. 14 (a) Comparison of the reflection performance of the semicircular and rectangular sections, $100(K_{RR} - K_{RS})/(K_{RS})$. K_{RS} is the reflection coefficient of the semicircular breakwater, while K_{RR} is the reflection coefficient of the rectangular breakwater. (b) Comparison of the transmission performance of the semicircular and rectangular sections, $100(K_{TS} - K_{TR})/(K_{TS})$. K_{TS} is the transmission coefficient of the semicircular breakwater, while K_{TR} is the transmission coefficient of the rectangular breakwater. (c) Comparison of the dissipation performance of the semicircular and rectangular sections, $100(K_{DR} - K_{DS})/(K_{DS})$. K_{DS} is the dissipation coefficient of the semicircular breakwater, while K_{DR} is the dissipation coefficient of the rectangular breakwater

breakwater. Considering all the information provided in this section, the rectangular geometries seem to have a better overall performance than the semicircular section.
To summarize, quantitatively the transmission coefficients K_T for rectangular breakwaters are lower than that for the semicircular breakwaters. But the reflection and diffusion coefficients (K_R and K_D) are 5-15% and 3-23% higher for rectangular barriers, respectively. This Indicates that the performance of rectangular breakwaters is better compared to semicircular barriers when interacting with solitary waves.

8. Conclusions

In this paper, a numerical model has been applied to compare the performances of the rectangular and semicircular submerged breakwaters. Since these submerged breakwaters are installed in waters of intermediate depth, the Boussinesq equations have been used to simulate the interaction of the solitary wave with submerged breakwaters. The first order Adams-Bash forth-Moulton Predictor-Corrector method is applied for solving the governing equations together with solid wall and spongy boundary conditions.

To validate the model, five tests have been considered and the numerical results have been compared against analytical and experimental data. First, solitary wave propagation has been simulated for a long distance with a constant depth and the results have been compared with analytical data. Wave propagation for a long time range does not produce a change in its shape indicating conservative and stability properties of the numerical schemes. second, to assess the nonlinear terms of the model, solitary wave propagation has been considered on a beach with a variable slope and the results have been compared against experimental data. Fairly good agreement of the results indicates that the model is capable of simulating the wave run-up on the beach of variable slope and nonlinear effects with desirable accuracy. Third, in addition to modeling the nonlinear terms, wave propagation velocity and the reflecting boundary condition is analyzed. In this test, after runup on the slope, the wave collides with the solid wall and gets reflected. This, in turn, reveals that the model has good performance in simulating incident waves and its reflection. However, the slight difference between the numerical results and experimental data can be attributed to the fact that the numerical model does not involve any energy absorption by the solid wall, while in the experimental model, part of the wave energy gets absorbed by the solid wall. This causes the minimal difference between the wave heights by numerical and experimental models.

Next, in order to compare the performance of the intended submerged breakwaters, two tests have been considered for the simulation of a solitary wave interacting with interaction rectangular and semicircular submerged breakwaters. A comparison of our computed results against experimental data shows that the model performs well in simulating the interaction of waves with obstacles. After validating the model, an extensive set of parametric studies has been conducted on the RTD performance of rectangular and semicircular sections with various dimensions and different wave heights. The RTD coefficient charts related to each of the submerged breakwater structures presented in this work (Figs. 11 and 12) can be a suitable reference for engineering design. Another notable observation in our numerical study is the dissipative effect of the non-dissipative model equations. This is due to the nonenergy conserving transmission and reflection coefficients (K_R and K_T).

Our comparison of the performance of the rectangular and semicircular breakwaters shows that the rectangular sections perform up to 15% better than the semicircular sections in reflecting waves.

Also, the dissipative effects of the rectangular sections are up to 23% better than the semicircular sections. On the other hand, it is observed that by increasing the height of the breakwater, the effects of geometry become more and more visible. By comparing the transmission coefficients of both barriers with different dimensions and waves, one can say that by increasing the wave height, the difference between transmission coefficients of the two sections increases and rectangular sections have a better performance. The transmission coefficients K_T for rectangular breakwater shows the better performance up to 2.47% better than that for the semicircular breakwaters. Based on the results reported here, the conclusion is that in the hydrodynamical context the rectangular section has a better overall performance than the circular section. Generalization of our approach to multiple submerged obstacles (Zhou and Li 2012) may be possible but will not be discussed here. Finally, in many circumstances solitary waves can be utilized to represent certain behavior of long waves (leading waves of tsunami, for instance) in ocean. Performing numerical simulations for other types of waves, such as periodic and irregular waves, and comparison with our present calculations could yield more meaningful results. Such a theme can be the subject of future study.

References

Allsop, N.W.H. (1983), "Low-crest breakwaters, studies in random waves", *Proceedings of the 83th Conference of coastal structure (Arlington, United States, ASCE)*, 94-107.

Beji, S. and Battjes, J.A. (1993), "Experimental investigation of wave propagation over a bar", *J. Coastal Eng*., 19(1-2), 151-162.

Beji, S. and Battjes, J.A. (1994), "Numerical simulation of nonlinear-wave propagation over a bar", *J. Coastal Eng*., **23**(1-2), 1-16.

Beji, S. and Nadaoka, K. (1996), "A formal derivation and numerical modelling of the improved Boussinesq equations for varying depth", *J. Coastal Eng*., **23**, 691-704.

Bogucki, D., Haus, B.K. and Shao, M. (2020), February. The dissipation of energy beneath non-breaking waves. In *Ocean Sciences Meeting 2020*. AGU.

Cheng, M.H. and Hsu, J.R.C. (2013), "Effect of frontal slope on waveform evolution of a depression interfacial solitary wave across a trapezoidal obstacle", *J. Coastal Eng*., **59**, 164-178.

Cheng, S.; Liu, S. and Zheng, Y. (2003), "Application study on submerged breakwaters used for coastal protection", *Proceedings of the International Conference Estuaries and coast*, Hangzhou, China.

Cooker, M.J.; Peregrine, D.H.; Vidal, C. and Dold, J.W. (1990), "The interaction between a solitary wave and a submerged semicircular cylinder", *J. Fluid Mech*., **215**, 1-22.

Dean, R.G., Chen, R. and Browder, A.E. (1997), "Full scale monitoring study of asubmerged breakwater, Palm Beach, Florida, USA", *J. Coastal Eng*., **29**, 291-315.

Dick, T.M. and Brebner, A. (1968), "Solid and permeable submerged breakwaters", *Proceedings of the 11th International Conference on Coastal Engineering*, Kingston, Canada.

Dodd, N. (1997), "A numerical model of wave run-up, overtopping and regeneration", *J. Waterway, Port, Coastal, and Ocean Eng.*, **124**(2), 73-81.

Ghadimi, P. and Lamouki, M.B.P. (2017), Finite difference simulation of regular wave propagation over natural beach and composite barriers by Nwogu's extended Boussinesq equations", *Progress in Computational Fluid Dynamics, J*., **17**(4), 212-220.

Ghiasian, M., Carrick, J., Lirman, D., Baker, A., Ruiz-Merchan, J., Amendolara, J., Hasu, B. and RhodeBarbarigos, L. (2019), "Exploring coral reef restoration for wave-energy dissipation through experimental laboratory testing", Conf. in Coastal Structures.

Ghiasian, M., Rossini, M., Amendolara, J. Hasu, B., Nolan, S., Nanni, A., Bel Had Ali, N. and RhodeBarbarigos, L. (2019), "Test-driven design of an efficient and sustainable seawall structure", Conf. in Coastal Structures.

Grilli, S.T. (1997), "Fully nonlinear potential flow models used for long wave run-up prediction, long-wave run-up models", (Eds., Yeh, P.H.; Liu, P., and Synolakis, C.), Long-Wave Runup Models. World Scientific, Singapore.

Grilli, S.T.; Losada, M.A. and Martin, F. (1994), "Characteristics of solitary wave breaking induced by breakwaters", *J. Waterway, Port, Coastal and Ocean Eng*., **120**(1), 74-92.

Hsu, T.W.; Hsieh, C.M. and Hwang, R.R. (2004), "Using RANS to simulate vortex generation and dissipation around impermeable submerged double breakwaters", *J. Coast. Eng*., **51**(7), 557-579.

Jabbari, M.H., Ghadimi, P., Masoudi, A. and Baradaran, M.R. (2013), "Numerical modeling of the interaction of solitary waves and submerged breakwaters with sharp vertical edges using one-dimensional Beji & Nadaoka extended Boussinesq equations", *Int. J. Oceanography*, 2013.

Ji, C.Y., Yu-Chan, G.U.O., Cui, J., Yuan, Z.M. and Ma, X.J. (2016), "3D experimental study on a cylindrical floating breakwater system", *Ocean Eng*., **125**, 38-50.

Johnson, R.S. (1972), "Some numerical solutions of a variable coefficient Kortweg-de Vries equation (with application to solitary wave development on a shelf)", *J. Fluid Mech*., **54**, 81-91.

Ketabdari, M.J., Lamouki, M.B.P. and Moghaddasi, A. (2015), "Effects of discontinuous submerged breakwater on water surface elevation", *Ocean Syst. Eng*., **5**(4), 319-329.

Ketabdari, M.J. and Lamouki, M.B.P. (2014), "Numerical modelling of induced rip currents by discontinuous submerged breakwaters", *Int. J. Marine Sci. Eng*., **4**(1), 15-24.

Lee, C. and Jung, T.H. (2018), "Extended Boussinesq equations for waves in porous media", *Coast. Eng*., **139**, 85-97.

Lee, K.H. and Mizutani, N. (2008), "Experimental study on scour occurring at a vertical impermeable submerged breakwater", *J. Appl. Ocean Res*., **30**(2), 92-99.

Li, Y.S.; Liu, S.X., Yu, Y.X. and Lai, G.Z. (1999), "Numerical modeling of Boussinesq equations by finite element method", *J. Coast. Eng*., **37**, 97-122.

Lin, P. (2004), "A numerical study of solitary wave interaction with rectangular obstacles", *J. Coast. Eng*., **51**, 35-51.

Lin, P. and Karunarathna, S. (2007), "Numerical study of solitary wave interaction with porous breakwaters", *J. Waterw. Port Coast. Ocean Eng*., 352-363.

Lin, P. and Man, C. (2007), "A staggered-grid numerical algorithm for the extended boussinesq equations", *J. Appl. Math. Model*., **31**, 349-368.

Liu, Y. and Yue, D.K.P. (1998), "On generalized Bragg scattering of surface -waves by bottom ripples", *J. Fluid Mech*., **356**, 297- 326.

Losada, M.A.; Vidal, C. and Medina, R. (1989), "Experimental study of the evolution of a solitary wave at an abrupt junction", *J. Geophys. Res*., **94**(10), 14557-14566.

Lynett, P.J., Liu, P.L.F., Losada, I.J. and Vidal, C. (2000), "Solitary wave interaction with porous breakwaters", *J. Waterw. Port Coast. Ocean Eng*., **126**(6), 314-322.

Madsen, P.A., Murray, R. and Sørensen, O.R. (1991), "A new form of the Boussinesq equations with improved linear dispersion characteristics: Part 1", *J. Coast. Eng*., **15**, 371-388.

Madsen, P.A. and Sørensen, O.R. (1992), "A new form of the Boussinesq equations with improved linear dispersion characteristics. Part 2: A slowly varying bathymetry", *J. Coast. Eng*., **18**, 183-204.

McCowan, J. (1894), "XXXIX. On the highest wave of permanent type", *The London, Edinburgh, and Dublin Philosophical Magazine J. Sci*., **38**(233), 351-358.

Mei, C.C. (1985), "Scattering of solitary wave at abrupt junction", *J. Waterw. Port Coast. Ocean Eng*., **111**(2), 319-328.

Miche, M. (1944), "Mouvements ondulatoires de la mer en profondeur constante ou décroissante", Annales de Ponts et Chaussées, (1) 26-78, (2) 270-292, (3) 369-406.

Murashige, S. and Wu, T.Y. (2010), "Dwarf solitary waves and low tsunamis", *J. Hydrodynamic*, **22**(5), 960-968.

Newman, J.N. (1965), "Propagation of water waves past long two dimensional obstacles", *J. Fluid Mech*., **23**, 23-29.

Nwogu, O. (1993), "An alternative form of the Boussinesq equations for nearshore wave propagation", *J.*

Waterw. Port Coast. Ocean Eng., **119**, 618-638.
Peregrine, D.H. (1967), "Long waves on a beach", *J. Fluid Mech*., **27**, 815-827.
Raman, H.; Shankar, J. and Dattatri, J. (1977), "Submerged Breakwater", *Central Board of Irrigation and Power J*., **34**, 205-212.
Russell, J.S. (1844), "Report on waves", *Proceedings of the 14th Meeting British Association for Advancement of Science*, London, England.
Seabra-Santo, J.S., Renouardd, P. and Tempervillage, M. (1987), "Numerical and experimental study of the transformation of a solitary wave over a shelf or isolated obstacle", *J. Fluid Mech*., **176**, 117-134.
Shiah, J.B. and Mingham, C.G. (2009), "A temporally second-order accurate Godunov-type scheme for solving the extend Boussinesq equations", *J. Coast. Eng*., **56**, 32-45.
Tappert, F.D. and Zabusky, N.J. (1971), "Gradient-induced fission of solitons", *J. Phys. Review Lett*., **27**(26), 1774-1776.
Tonelli, M. and Petti, M. (2009), "Hybrid finite volume–finite difference scheme for 2DH improved Boussinesq equation", *J. Coast. Eng*., **56**, 609-620.
Tsai, C.Y., Hsu, T.W., Ou, S.H., Lin, J.F. and Hsu, L.C. (2005), "A solitary wave propagating over a submerged breakwater with high Reynolds number", *Proceedings of the 27th Ocean Engineering Conference*, Taiwan, China.
Walkley, M. (1999), A numerical method for extended Boussinesq shallow-water wave equations. Leeds, The England: University of Leeds, Ph.D. thesis, 185p.
Wang, Y., Yin, Z., Liu, Y., Yu, N. and Zou, W. (2019), "Numerical investigation on combined wave damping effect of pneumatic breakwater and submerged breakwater", *Int. J. Naval Architect. Ocean Eng*., **11**(1), 314-328.
Wei, G. and Kirby, J.T. (1995), "Time-dependent numerical code for extended Boussinesq equations", *J. Waterw. Port Coast. Ocean Eng*., 121, 251–261.
Wei, G., Kirby, J.T., Grilli, S.T. and Subramanya, R. (1995), "A fully nonlinearBoussinesq model for surface waves. Part 1: Highly nonlinear unsteady waves", *J. Fluid Mech*., **294**, 71-92.
Wu, Y.T. and Hsiao, S.C. (2013), "Propagation of solitary waves over a submerged permeable breakwater", *J. Coast. Eng*., **81**, 1-18.
Wu, Y.T. and Hsiao, S.C. (2017), "Propagation of solitary waves over double submerged barriers", *Water*, **9**(12), 917.
Xie, J.J. and Liu, H.W. (2013), "Analytical study for linear wave transformation by a trapezoidal breakwater or channel", *J. Ocean Eng*., **64**, 49-59.
Yuan, D. and Tao, J. (2003), "Wave forces on submerged, alternately submerged, and emerged semicircular breakwaters", *J. Coast. Eng*., **48**(2), 75-93.
Young, D.M. and Testik, F.Y. (2011), "Wave reflection by submerged vertical and semicircular breakwaters", *J. Ocean Eng*., **38**(10), 1269-1276.
Young, D.M. and Testik, F.Y. (2009), "Onshore scour characteristics around submerged vertical and semicircular breakwaters", *J. Coast. Eng*., **56**(8), 868-875.
Zhang M, Qiao H, Xu Y. (2017), "Numerical simulation of solitary wave propagation in a vegetated channel using an extended Boussinesq model", *J. Mar. Sci. Technol*., **25**(1), 119-128.
Zhou, Q., Zhan, J.M. and Li, Y.S. (2012), "Numerical study of interaction between solitary wave and two submerged obstacles in tandem", *J. Coast. Res*., **30**(5), 975-992.